A MODELING STUDY FOR THE PIN ASSISTED PULTRUSION OF POROUS SUBSTRATES

Nickolas D. Polychronopoulos and T. D. Papathanasiou

Department of Mechanical Engineering
University of Thessaly
Volos, GR-38334, Greece
e-mail: npolychron@mie.uth.gr ; web page: www.mie.uth.gr

Keywords: Computational Mechanics, porous, fibers, pultrusion, composites

Abstract. *We report on the results of a two dimensional numerical study using OpenFOAM, of the process of infiltration of a homogeneous porous substrate, moving over a stationary solid pin, by an incompressible, isothermal and Newtonian fluid. The motion of the substrate relative to the cylindrical pin causes a pressure build-up in the wedge-shaped region separating them, which forces the fluid to penetrate into the porous material. The analysis assumes Stokes flow outside the substrate and uses Brinkman's equation to describe the flow inside the substrate. The structure of the flow field is characterized by the combination of a drag and an opposing pressure-driven flow, the latter caused by the above mentioned pressure build-up in the wedge. The amount of fluid penetrating into the substrate is found to be affected by various parameters such as the pulling speed, substrate permeability, pin diameter and substrate thickness. Based on large numbers of simulations, we correlate the achieved impregnation depth to the above parameters and propose a previously unavailable quantitative relationships expressing the above dependencies.*

1 INTRODUCTION

Polymeric fibrous composites consist of thermoplastic or thermoset polymer matrices reinforced by various types of fibers. Several composites manufacturing technologies have been developed over the past years, such as pultrusion, resin transfer molding and resin infusion with many applications in the aerospace, automotive and construction industries. A key step in the above processes is the resin infiltration of the reinforcement, having a critical and often detrimental effect on the quality and subsequent performance of the final manufactured product. In fact, failure of composite components is most often linked to poor/incomplete resin infiltration of the fibrous substrate. To facilitate this, besides control of the architecture (and thus permeability) of the fibrous preform/substrate, pressure is applied. In the pultrusion process of interest to this study, namely pin-assisted pultrusion, bundles of fibers are pulled through a die and over an array of cylindrical pins located inside a pool of polymeric resin. During the pulling of the roving over and around each pin, a small wedge-shaped region is formed between the roving and the pin. The pressure generated in this region forces the fluid to penetrate into the porous substrate while the pulling laterally spreads the fibrous roving making the fluid penetration even easier. Usage of different numbers of pins can accomplish the desired final degree of impregnation.

Many approaches followed so far have mostly utilized a one-dimensional form of Darcy's law [1-4] or proposed models which relate the generated pressure with the applied roving's tension [5,6]. The details of the fluid mechanics of the process in the region near the roving-pin contact are central to any analysis of predictive value and have not yet been fully understood. No study has appeared in the technical literature in which the two-dimensional nature of the flow in the entire region where the disturbance introduced by the pin is felt or the details of the intra-roving pressure development (by utilizing Brinkman's equation) have been considered. To fill this gap, we analyze the results of a large number of 2D simulations using the OpenFOAM software to relate the resin infiltration depth to measurable process parameters. We employ Brinkman's equation for the flow in the porous substrate, assuming the latter to be homogeneous and isotropic, and Stokes equation for the flow in the region occupied by the resin.

2 MODEL FORMULATION

Our analysis considers a single-pin process in which resin infiltration occurs only within the wedge- shaped region forming prior to zero tangency point. This ignores any additional infiltration that might occur in the small region in which the roving is in near-contact with the pin. Since the extent of this zone is unknown, this is a

reasonable assumption, avoiding the need to introduce arbitrary variables in the analysis. This assumption is also in line with earlier work on the topic (e.g [4]). While any such secondary infiltration is not considered, our analysis takes full account of the presence of a large (compared to the dimensions of the pin) resin pool surrounding it. Finally, it is known that as it comes in contact with the pin, a fibrous roving will spread laterally (due to leakage flow) over the pin length resulting in a decrease of its thickness as well as in a change in its microstructure. This spreading is also beyond the scope of this study. Summarizing, we focus on the effect the hydrodynamics within the fluid wedge have on the extent of resin infiltration, taking full account of the 2D nature of this flow and of the presence of a large resin bath. The flow in the resin pool is modeled using the continuity (eqn 1) and Stokes equation (eqn2) as

$$\nabla \cdot \mathbf{U} = 0 \tag{1}$$

$$0 = \nabla p + \mu \nabla^2 \mathbf{U} \tag{2}$$

and is regarded as steady-state, isothermal, incompressible and Newtonian, while for the flow inside the porous substrate the Brinkman equation

$$\nabla p = -\mu \mathbf{K}^{-1} \cdot \mathbf{U} + \mu_e \nabla^2 \mathbf{U} \tag{3}$$

is utilized where p the pressure, $\mathbf{U}$ the velocity, $\mathbf{K}$ the permeability tensor and μ, μ_e the fluid and the effective viscosity respectively. A value of μ=1000 Pa·s is used for the resin viscosity. Following earlier studies of fluid flow in porous media with Brinkman's equation we choose $\mu_e=\mu$ [7-9]. The porous substrate is regarded as isotropic. Brinkman's equation for non-isotropic porous medium and thus use of a second-order permeability tensor can be easily implemented.

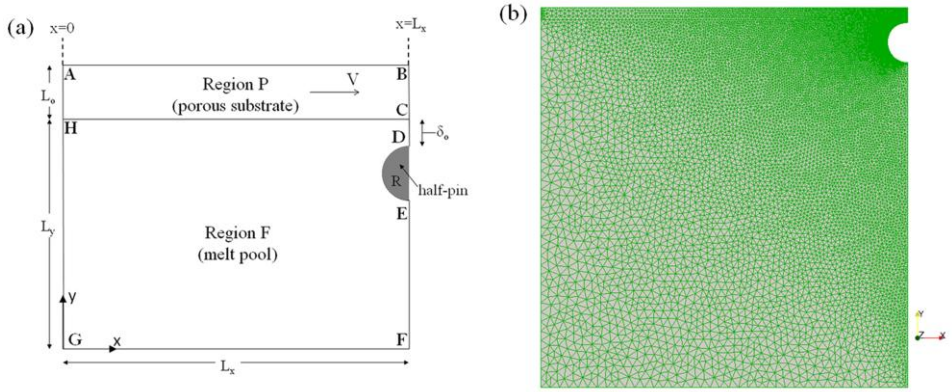

Figure 1. Schematic representation (a) and computational flow domain utilized (b).

The geometrical domain utilized is shown in Figure 1a. A pre-impregrated zone of thickness L_o, the value of which varies, is assumed to exist. This zone moves with speed V (pulling speed) in the x-direction as denoted in Fig. 1a. The-top boundary (boundary AB in Figure 1a) represents the infiltration profile of the fluid. The resin pool (region F) is defined so that L_y>>R and L_x>>R . In this way, the boundary conditions imposed on the corresponding boundaries (that is boundaries FG and GH) will have little, if any, effect to the behavior of the flow in the wedge-shaped region forming between the pin and the porous substrate. A constant value is utilized for the horizontal distance L_x (L_x=90 mm). The vertical distance L_y can vary, since we perform simulations for various values of the pin radius R and the gap δ_o as L_y=84.445+R+δ_o mm. In Figure 1b the computational domain employed is shown.

We use a decoupled iterative predictor-corrector procedure to calculate the amount of fluid penetrating the porous substrate. By such we assume that the shape of boundary AB (which expresses the infiltration profile) in Figure 1a can change the final shape of which will be determined by requiring that at steady state the fluid velocity Un across that boundary $U_n = -U_x \cdot \sin\theta + U_y \cdot \cos\theta$ is zero. This results in

$$\tan\theta \equiv \frac{dy}{dx} = \frac{U_y}{U_x} \tag{4}$$

where dy/dx is the local slope of line AB, U_y is the velocity in the transverse direction (y-direction) and U_x the

velocity in the *x*-direction. To determine the shape of the infiltration profile, the continuity, Stokes and Brinkman equations are solved for an initial configuration, for example with AB as a straight line. At the end of this step (predictor), the velocity and pressure fields are known everywhere, including on line AB. The corrector step involves the correction of the shape of boundary AB, based on integration of eqn 4. A rigorous description about this method can be find in [10]. In the past a similar approach was followed to quantify the amount of spreading a highly viscous experiences when it passes two co-cotating rollers [11].

3 RESULTS AND DISCUSSION

Results for the final convergent shape of the boundary AB, assuming μ=1000 Pa·s, L_o=1mm and δ_o=0.544 mm, for different permeability values (K=10^{-6} m^2 to K=10^{-8} m^2) are shown in Fig. 2. The final infiltration depth ΔL_f is the vertical distance between point A and point B_i and the maximum distance between the pin and the substrate is located at x=0.085 m (note that R=0.005m). For the cases with highly permeable substrate (e.g. K=10^{-6} m^2) and for low thickness of the pre-impregnated zone (e.g. L_o=1 mm) a maximum of 7 iterations were needed to obtain convergence of the order of 10^{-6}. In the cases of low K (e.g. K=10^{-8} m^2) a maximum of 3 iterations were needed, even for the cases of low L_o (e.g. L_o=1 mm). We observe that the maximum infiltration depth ΔL_f is located at the symmetry axis of the pin. It is interesting to also note that, as is evident in the case of K=10^{-6} m^2, a significant amount of fluid infiltrates the substrate well ahead of the pin.

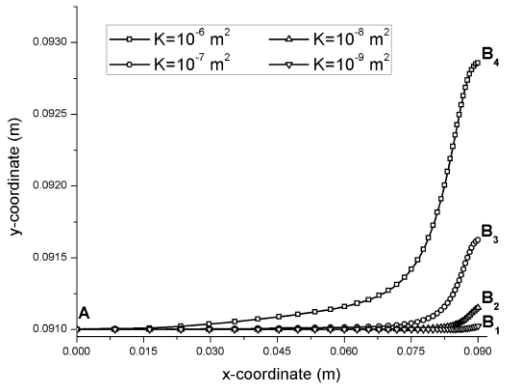

Figure 2. Steady state shape of the resin infiltration profile (curves AB_4 to AB_1) for K = 10^{-6}, 10^{-7}, 10^{-8} and 10^{-9} m^2 , respectively. L_o = 1 mm, R = 5 mm, d_o = 0.544 mm, V = 0.15 m/s, μ=1000 Pa.s.

The permeability of the porous substrate has a significant effect on the pressure field. This is shown in Fig. 3a for K=10^{-9} m^2 and in Fig. 3b for K=10^{-7} m^2. Evidently, for K=10^{-9} m^2 the maximum pressure is observed to occur at the zero-tangency point (i.e. minimum distance between the pin and porous substrate). However, when the permeability of the substrate increases, the local pressure maximum shifts away from the zero-tangency point - as shown in Fig. 3b. For this reason the resin starts infiltrating even before reaching the wedge-shaped region – observe the infiltration profiles shown in Fig. 2. An even larger shift of the pressure maximum to the left is observed for K=10^{-6} m^2, at which value the infiltration of the substrate appears to take place far ahead of the pin (profile AB_4 in Fig. 2). It should be pointed out that earlier approaches to quantify the infiltration of the porous substrate assume that pressure build-up and resin infiltration take place only in the wedge-shaped region formed between the substrate and the pin. This essentially implies that the pressure at distances beyond one pin radius from the zero tangency point must be zero. The present two-dimensional approach suggests that at high substrate permeabilities significant infiltration may occur well ahead of the pin.

In a previous study [10] it was rigorously elucidated that the penetration depth may be affected by different operating and geometric parameters expressed via dimensionless quantities such as, $\sqrt{\delta_o L_o}$, $L_o/\sqrt{K}$ and L_o/R for a single pin process. Such a scaling procedure was developed by examining separately each time a specific parameter and the suggested scaling was a direct and natural consequence of raw computational data obtained. A very significant parameter which was neglected in the correlation of the obtained numerical data is the generated pressure P in the wedge shaped region formed between the pin and the substrate. It is convenient to express this pressure in terms of a average generated pressure P_{av} as

$$P_{av} = \frac{1}{L_x}\int_{L_x} P(x)dx \tag{5}$$

assuming that this average pressure is applied over a distance L_x=R. We perform simulations for a wide range of process parameters (μ, V, L_o, δ_o, K, R), and for each produced penetration depth h_f we calculate the average pressure P_{av} based on eqn 5. Based on the dimensionless scaling arguments discussed previously, the above-mentioned process parameters may be grouped together into a single universal dimensionless parameter as

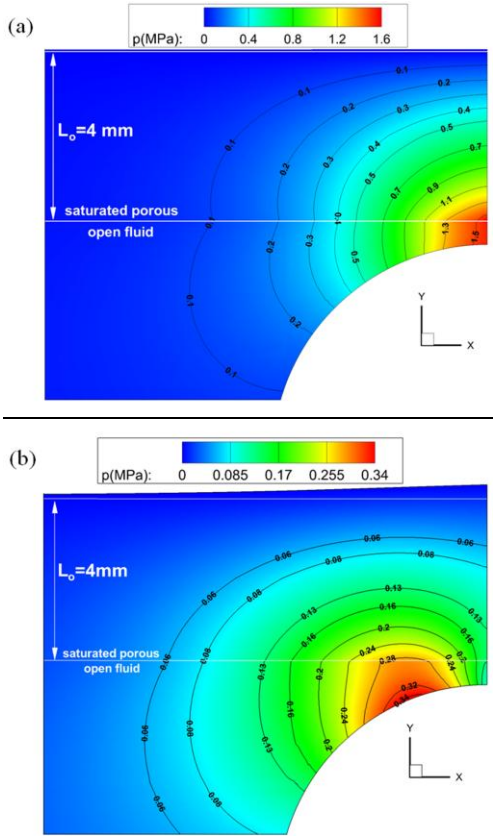

Figure 3. Pressure field near the wedge-shaped region formed between the pin and the porous medium for (a) K = 10^{-9} m^2 , L_o = 4 mm, R = 5 mm, V = 0.15 m/s and μ = 1000 Pa.s; and (b) K = 10^{-7} m^2 , L_o = 4 mm, R = 5 mm, V = 0.15 m/s and μ = 1000 Pa.s. Notice that the small region above L_o corresponds to ΔL_f.

($\mu L_o V/KP_{av}$)·(δ_o/R). By doing so and as shown in Figure 4 the obtained data appear to produce a generic trend as they into the same region which a relatively small scatter. This trend may be sufficiently be expressed by fitting the produced data as

$$h_f = \frac{A}{1 + B\left(\frac{\mu V L_o}{P_{av} K}\frac{\delta_o}{R}\right)^C} \tag{6}$$

where A=8.21×10^{-4} m, B=0.879 and C=1.2 are fitted parameters. The global curve expressed by Equation (6) may give an estimate of the penetration depth at distinguishably different types of conditions by which impregnation may take place. Essentially, the global dimensionless group could be regarded as the ratio of viscous resistance of fluid flow to the fluid penetration by permeation multiplied by a scaled form the pin radius which expresses the geometric parameters of the process. When the viscous forces dominate the flow penetration by permeation is small while the opposite takes place when the viscous forces are low. For cases where the viscous force is balanced by the fluid penetration due to permeation force increasing the pin radius will increase

the fluid infiltration into the porous. Moreover, it can be concluded that the fluid viscosity, production rate (i.e. pulling speed V), permeability of the substrate and pin radius can be adjusted accordingly for the production of similar quality impregnated fibrous products. It should also be pointed out that the finite value A=8.21×10^{-4} m of

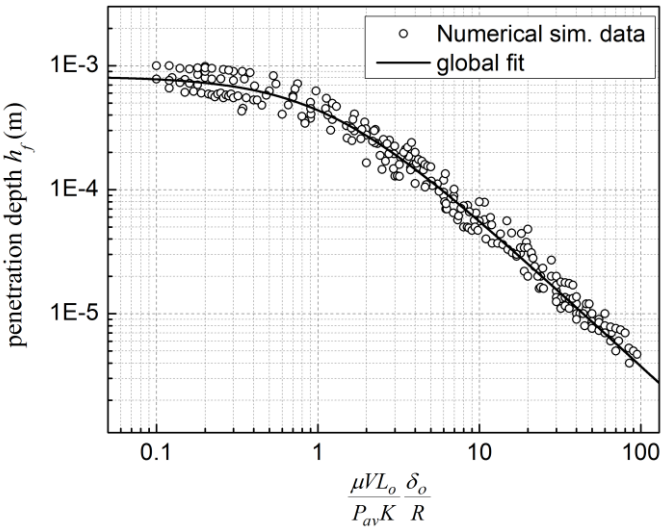

Figure 4. Effect of the global dimensionless parameter on the penetration depth h_f.

eqn 6 corresponds to the limit of a dry substrate. Our results indicate that at this limiting case the infiltration depth is essentially not affected by the process conditions. While this is not the case for the real pin-assisted process we assume that at this limiting condition the infiltration depth remains constant as an initial approximation for the subsequent study of multi-pin arrangements at which the substrate passing over the next pin is not dry. The above equation (eqn. 6) can be easily utilized in a recurrence form for the more realistic multi-pin arrangement system where a sequential array of pins is frequently employed.

4 CONCLUSIONS

We have presented a two dimensional numerical approach using the Stokes and Brinkman equations to describe the pin assisted pultrusion process as a fibrous substrate is dragged over a single rigid stationary cylindrical pin. By such the movement causes a significant pressure build up in the space separating the substrate and the fluid which forces the fluid to penetrate the permeable substrate. Our two dimensional results indicate that permeability chiefly controls the relative penetration amounts and alters to some extend the pressure distribution by forcing the fluid to enter the substrate far before it approaches the pin as elucidated for highly permeable substrates. The most important feature of the present analysis is underlined by a proposed process model which is able to describe the process in a generic form. While the computational experiments were performed by isolating each process parameter at a time, when reasonably scaled into a dimensionless group of physical meaning, they fall into the same curve (with small scatter). Use of such a model may be easily transformed into an even more applicable recurrence formula to quantify infiltration depths in pultrusion processes were a sequential amount of pins is employed and frequently used in the pin-assisted pultrusion technology.

REFERENCES

[1] Bijsterbosch, H., and Gaymans, R.J., (1993), "Impregnation of glass rovings with a polyamide melt. Part 1: Impregnation bath", *Composites Manufacturing*, Vol. 4, pp. 85–92.

[2] Gaymans, R.J., and Wevers E., (1998), "Impregnation of a glass fiber roving with a polypropylene melt in a pin assisted process", *Composites Part A: Applied Science & Manufacturing*, Vol. 29, pp. 663–670.

[3] Bates, P.J., and Charrier, J.M., (1999), "Effect of process parameters on melt impregnation of glass roving", *Journal of Thermoplastic Composite Materials*, Vol. 12, pp. 276–296.

[4] Bates, P.J., and Zou, X.P., (2002), "Polymer melt impregnation of glass roving.", International Polymer Processing, Vol. 17, pp. 376–386.

[5] Bates, P.J., and Charrier J.M., (2000), "Pulling tension monitoring during the melt impregnation of glass roving." *Polymer Composites*, Vol. 21, pp.104–113.

[6] Bates, P.J., Kendall J., Taylor D, and Cunningham M., (2002), "Pressure build-up during melt impregnation.", *Composites Science and Technology*, Vol. 62, pp. 379–384.

[7] Ranganathan, S., Phelan, F.R., and Advani S.G., (1996), "A generalized model for the transverse fluid permeability in unidirectional fibrous media.", *Polymer Composites* Vol. 17, pp. 222–230.

[8] Yu, B., James Lee L., (2000), "A simplified in-plane permeability model for textile fabrics.", *Polymer Composites*, Vol. 21, pp. 660–685.

[9] Ngo ND, Tamma KK., (2001), "Microscale permeability predictions of porous fibrous media." *International Journal of Heat and Mass Transfer*, Vol. 44, pp. 3135-3145.

[10] Polychronopoulos, N.D., and Papathanasiou T.D., (2015), "Pin Assisted Resin Infiltration of porous substrates.", *Composites Part A: Applied Science and Manufacturing*, Vol.71, pp. 126-135.

[11] Polychronopoulos N.D., Sarris I.E., and Papathanasiou T.D., (2014), "3D features in the calendering of thermoplastics: A computational investigation", *Polymer Engineering Science*, Vol. 54, pp. 1712-1722.